Chapter 5 $MoSe_2$ based Nanomaterials as Electrodes for Electrolyzer

5.1 Introduction

Hydrogen energy is an alternative to fossil fuels that has the potential to provide a cleaner and more sustainable source of energy in the form of combustion engines, fuel cells, and as a transportation fuel [160, 161]. Traditional industrial hydrogen production from natural gas reforming consumes significant nonrenewable energy and emits greenhouse gases like carbon dioxide. In contrast, electrochemical water splitting offers a sustainable and pollution-free approach to generate hydrogen. Electrochemical water splitting involves two half-cell reactions. First, HER: water is reduced at the cathode to produce hydrogen. Second, OER: water is oxidized at the anode to produce oxygen as shown in **Figure 5.1**.

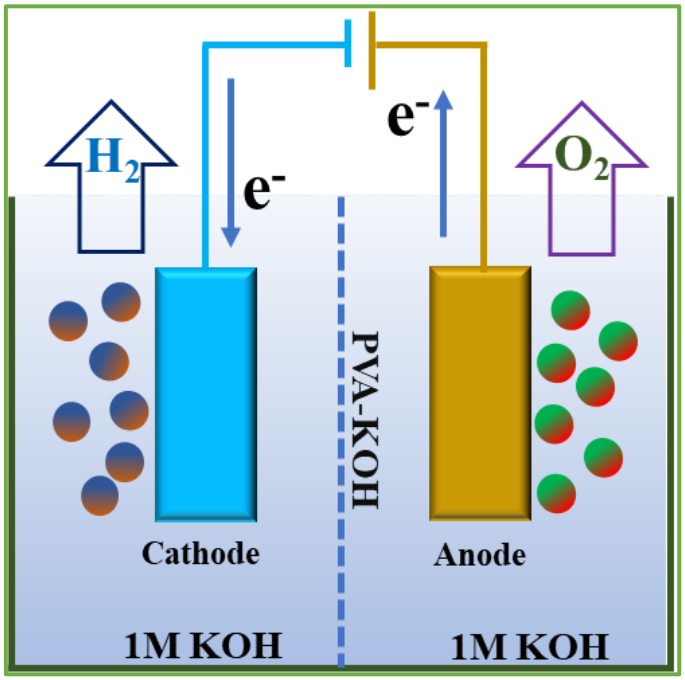

Figure 5.1 *Schematic diagram of overall water splitting.*

Traditionally, costly metals (such as Pt, Ir, and Ru) and metal oxides (like IrO_2 and RuO_2) are used as electrocatalysts to promote the HER and OER reactions, respectively, but their

expensiveness and limited availability prevent their widespread usage in real manufacturing. Concurrently achieving excellent performance in both the HER and OER using a single catalyst under the same electrolyte conditions is a challenging task. To address this issue, the research community is currently focussing on developing earth-abundant bifunctional electrocatalysts as promising replacements. The use of such catalysts in electrolyte-mediated overall water splitting systems has become a significant area of interest in current research. Transition metal dichalcogenides (TMDs) like $MoSe_2$, MoS_2, WS_2, and WSe_2, have garnered significant interest as electrocatalysts owing to their fascinating material characteristics such as chemical stability, tuneable electronic properties and catalytic activity [162-164]. The $MoSe_2$ has a relatively low Gibbs free energy with a value of ΔG_H around 0.05 eV, indicating its proximity to thermoneutrality. As a result, $MoSe_2$ demonstrates excellent catalytic activity in water splitting [165, 166]. The low electrical conductivity of catalyst-loaded substrate is a major issue due to its high interfacial charge resistance between catalyst and substrate. Two-electrode electrolysis of water is a matured system that achieves overall water splitting with high performance at low cell voltages. A few benefits of using electrolyzers include the ability to manufacture hydrogen right there, where it is needed, rather than needing to store it beforehand, and the fact that they are far less expensive than receiving gas in high-pressure cylinders. The slightly different ways that various electrolyzers operate are determined by the types of electrolyte materials that are utilized. Researchers have made significant progress in designing and developing bifunctional electrocatalysts with excellent performance. These catalysts enable efficient overall water splitting by minimizing the cell voltage and ensuring long-term stability. The direct in-situ growth of $MoSe_2$ on a conducting substrate such as CCP and Ni foam provides several advantages. Firstly, the conducting substrate provides excellent electrical conductivity and facilitates efficient charge transfer during electrocatalytic reactions, which can improve the overall water-splitting efficiency of $MoSe_2$ [167]. Secondly, the substrate can support anchoring

and stabilizing $MoSe_2$ nanostructures, preventing their agglomeration and ensuring the long-term stability of the catalyst. Furthermore, the substrates serve a dual purpose by functioning as a scaffold to facilitate the growth of $MoSe_2$, thereby facilitating the formation of targeted crystal structures that boast optimized catalytic activity [127, 168]. Metal doping or decorating over $MoSe_2$ nanostructures can indeed enhance their electrocatalytic activity. The incorporation of metal atoms (Ni, Co etc.) into $MoSe_2$ can significantly alter the electronic configuration of the reactive species. This alteration can enhance the conductivity and facilitate electron and mass transfer, thereby accelerating the catalytic activity. The limited number of active sites in $MoSe_2$ can reduce their overall electrocatalytic performance. But metal decoration over $MoSe_2$ can improve the electronic conductivity of $MoSe_2$ and generate defects, creating numerous reactive sites for catalytic reactions. Multiple investigations on $MoSe_2$ and other TMDs based electrodes for overall electrochemical water splitting have been demonstrated in recent years [52-57]. In general, electrodes are prepared by using binders to hold the catalyst on the electrode substrate; however, they hinder the catalyst's performance due to a reduction in the electrode's effective surface area and electrical conductivity. Hence, developing binder-free electrodes is required for high-performance electrolyzers [33].

5.1.1 Types of electrolyzer

All existing technology operates on the same electrolysis concept. Nonetheless, there are a number of physical, chemical, and electrochemical differences between the methods. In the electrolyzer, there are four primary categories of electrolysis technologies such as alkaline electrolyzer, proton exchange membrane electrolyzer, solid oxide electrolysis cell electrolyzers and anion exchange membrane electrolyzers.

***Alkaline electrolyzer**:* Alkaline electrolyzer is well-established and widely used technology. At the moment, it represents over two thirds of the world's electrolyzer capacity. It employs electrocatalysts based electrodes and thick membranes to function. It is the least expensive

electrolyzer technology due to its straightforward and reasonably inexpensive stack and system design [169].

Proton exchange membrane electrolyzer: It fulfill the one-fifth of the global capacity. Proton exchange membrane electrolyzers operate on high pressure because of thin perfluoro sulfonic acid (PFSA) membranes, which translates to an efficiency of 80-90%. Its small size and straightforward design provide advantages when it comes to operating with intermittent demands, or quickly responding to fluctuating renewable electricity. Unfortunately, the acidic environment of PFSA necessitates the use of metal catalysts including ruthenium, iridium, and platinum, which raises the cost of the product considerably [170].

Solid oxide electrolysis cell electrolyzer: This method works best in areas with access to heat sources, such as nuclear or industrial facilities, as it uses heat to produce hydrogen from steam where the temperatures lie between 500 and 850 °C. It has higher efficiency than other technologies but it is not suited to withstand load changes. The technology is still at the demonstration level [171].

***Anion exchange membrane electrolyzer*:** It operates between 1 and 30 bar of pressure at much lower temperatures between 50 to 60 °C. They combine the ease of use and great efficiency of electrolyzers with the less demanding circumstances of alkaline electrolyzers. It is the newest technology, currently only being commercialized by a small number of companies, and is being used at the big prototype level [172].

5.2 Performance evolution index for electrolyzer:

The overpotential, faradaic efficiency and catalytic durability are important parameters that evaluate the overall electrolyzer performance.

5.2.1 Overpotential (η)

The overpotential is a common measure used to assess the overall catalytic activity of an electrolyzer, which exceeds the thermodynamic potential. The overpotential is the least amount of potential needed to produce oxygen/hydrogen on the respective surface of the electrocatalyst. The correlation between the overpotential and the overall potential is given by following **equation 5.1**.

$$E_{op} = 1.23 + iR + \eta \tag{5.1}$$

Where E_{op} is the overall potential of electrochemical reactions and iR is the ohmic potential drop due to the resistance of ion flow in the electrolyte. The 1.23 is the reversible thermodynamical potential of water, and η is an overpotential which is estimated by the polarization curve evaluated using LSV measurements.

5.2.2 Faradaic efficiency

The Faradic efficiency is a crucial parameter for evaluating the electrocatalytic performance of a catalyst in OER or HER for overall water splitting. The Faradic efficiency of the respective gas is calculated as the ratio of the experimentally evolved gas (H_2 or O_2) to the theoretically expected gas based on the electrochemical reactions using the following **equation 5.2** [173].

$$Faradaic\ efficiency = \frac{Experimentally\ gas\ evolved}{Theoratically\ gas\ evolved} \times 100\% \tag{5.2}$$

The ideal gas law is applied to calculate the molar volume of the gas evolved by following **equation 5.3** [174].

$$Theoratically\ gas\ evolved = \frac{Q}{n \times F} = \frac{i \times t}{n \times F} \tag{5.3}$$

Where, Q is the total quantity of electric charge, n is the number of moles of electrons transferred during the reaction, F is Faraday's constant (96485.3 C mol^{-1}), i represents the current in ampere and t is the time in sec.

5.3 Reaction mechanism for overall water splitting:

Water splitting reaction in alkaline medium is divided into two half-cell reactions: Cathodic half-cell reaction (hydrogen evolution) and anodic half-cell reaction (oxygen evolution), showing water oxidation reaction [86]. In the HER, water is reduced at the cathode to produce hydrogen. The reaction is as follows:

$$2H_2O + 2e^- \rightarrow H_2 + 2OH^- \quad (5.4)$$

In the OER, water is oxidized at the anode to produce oxygen. The reaction is as follows:

$$4OH^- \rightarrow O_2 + H_2O + 4e^- \quad (5.5)$$

The net reaction for the overall process of water splitting is:

$$2H_2O \rightarrow 2H_2 + O_2 \quad (5.6)$$

5.4 Electrocatalysts for electrolyzer:

In electrolyzer, either bifunctional electrocatalysts, suitable for HER and OER are used as electrodes or otherwise, OER electrocatalyst is used as anode and HER electrocatalyst is used as cathode. The ideal electrode materials should have a fast charge transfer rate, a high number of active sites, and should be affordable, abundant, and sustainable. Noble metals/metal-oxides such as iridium oxide (IrO_2), ruthenium oxide (RuO_2) etc. are highly effective in oxygen evolution reaction activity, but their high cost and negative environmental impact limit their practical application. As a result, there is a significant research effort aimed at finding cost-effective, earth-abundant alternatives with high catalytic activity [90]. Majumdar *et al.* have discussed a study on the development of a heterostructure catalyst for efficient overall water splitting. They introduce a $MoSe_2$@$NiCo_2Se_4$ heterostructure as HER electrocatalyst and single atom iridium decorated $MoSe_2$@$NiCo_2Se_4$ heterostructure as OER electrocatalyst. They have investigated the electrolyzer performance using the $MoSe_2$@$NiCo_2Se_4$ as cathode and its Ir decorated counterpart as anode, showing the overpotential of 280 mV at a current density of 10

mA cm^{-2} [58]. Inta *et al.* discussed the performance of electrolyzer using a $Ni_{0.85}Se/MoSe_2$ interfacial structure as cathode for HER and $Ni_{0.75}Se$ as anode for the OER. It shows current density of 10 mA cm^{-2} at a cell potential of 1.7 V and high durability, indicating effective overall water splitting [59]. Li *et al.* have introduced a 1T/2H $MoSe_2$ over MXene heterostructure as a bifunctional electrocatalyst for efficient overall water splitting, showing overpotential of 410 mV at a current density of 10 mA cm^{-2} with 50 h of durability at 1.64 V. The high performance of the electrolyzer is attributed to the large number of electrochemical active sites of 1T/2H $MoSe_2$ and high conductivity of MXene nanosheets to facilitate charge transfer. Cogal *et al.* demonstrated cobalt doped $MoSe_2$@PANI as bifunctional electrocatalytic electrodes for overall water splitting in 1M KOH solution. It shows the overpotential of 590 mV at current density of 10 mA cm^{-2} due to conducting template helping in holding TMD nanosheets and high synergy between TMDs and Co metal.

5.5 Assembly of designed electrolyzer

An electrochemical overall water splitting device (alkaline electrolyzer) has been fabricated that uses $MoSe_2$ based ($MoSe_2$-CCP, $MoSe_2$-Ni foam, Ni-$MoSe_2$ (5%), Ni-$MoSe_2$ (10%) and Ni-$MoSe_2$ (20%) nanocomposites as electrodes. The two electrodes are taken of 1 cm x 1 cm dimensions and fixed both of the two electrolytic chambers. The electrolytic chamber was filled with alkaline electrolyte (1M KOH). Two electrode chambers are separated by PVA-KOH based membrane to avoid gas mixing.

The **Figure 5.2 (a)** shows the image of indigenously designed electrolyzer fabricated using acrylic sheet. The electrolyzer is a prototype with a total cell capacity of 8 mL for electrolyte and has two replaceable electrode support structures which serve as a support to cathode and anode. The cell has been equipped with connections to both $MoSe_2$ based cathode and anode. The electrodes power connection terminals are freely accessible from the outside. The electrode replacement is made exceedingly simple by the design of the device. The **Figure**

5.2 (b) shows the image of indigenously designed electrochemical electrolyzer along with gas collection arrangement via water displacement method. Electrolytic chamber is filled with aqueous 1M KOH solution.

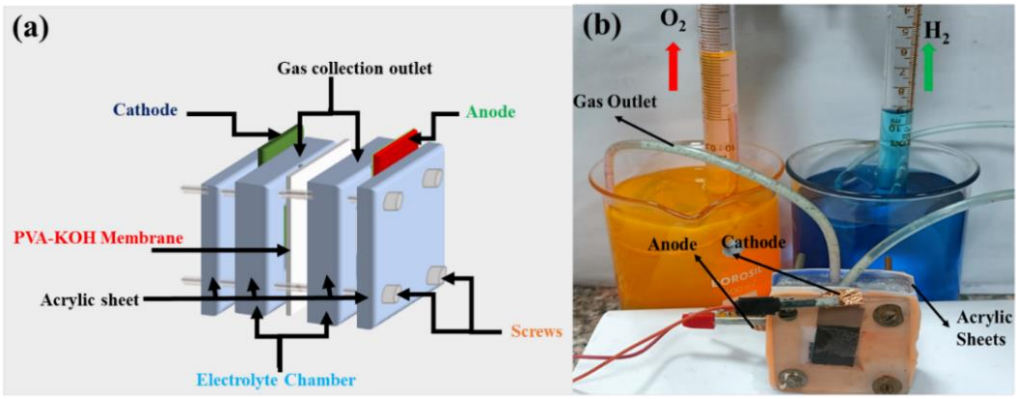

Figure 5.2 *(a) Schematic and (b) photograph of indigenously designed electrolyzer setup for production of H_2 and O_2.*

5.6 Result and discussion

5.6.1 *In-situ* grown $MoSe_2$ over different substrate as electrode for alkaline water electrolyzer

In this study, we have explored the hydrothermally synthesized in-situ grown $MoSe_2$ over conducting substrates (CCP and Ni foam) as binder-free electrode for electrochemical electrolyzer. The SEM and TEM studies reveal that $MoSe_2$ nanostructures have a well-defined, highly dense vertically grown wrinkled architecture with uniform distribution over CCP and Ni foam substrates, as shown in **Figure 3.3** of chapter 3. The XRD, Raman and FTIR studies of $MoSe_2$-CCP and $MoSe_2$-Ni foam have been discussed in **Figure 3.4** of chapter 3. They clearly indicate the uniform $MoSe_2$ phase over both substrates. The XPS study (**Figure 3.5** of chapter 3) of both electrodes shows the formation of hybrid 1T (20%) and 2H (80%) of $MoSe_2$ in $MoSe_2$-CCP electrode and 1T (34%) and 2H (66%) of $MoSe_2$ in $MoSe_2$-Ni foam electrode. It is also clear that $MoSe_2$-Ni foam has more metallic phase compared to $MoSe_2$-CCP, which may provide better catalytic response of $MoSe_2$-Ni foam. The ECSA study of $MoSe_2$-Ni foam show higher C_{dl} values of 58.2 mF cm^{-2} compare to $MoSe_2$-CCP (19.8 mF cm^{-2}) as shown in **Figure 3.6** of

chapter 3. The three electrode HER performance for both electrodes have been investigated in 1M KOH as previously shown in **Figure 3.7** of chapter 3. The performance of HER reveals that the $MoSe_2$-Ni foam shows lower η_{10} ~100 mV and Tafel slope ~73 mV dec^{-1} compared to $MoSe_2$-CCP (η_{10} ~ 220 mV, Tafel slope ~83 mV dec^{-1}). Similarly, for OER study, binder-free $MoSe_2$-Ni foam shows better OER performance (η_{50} ~292 mV and Tafel' slope ~20 mV dec^{-1}) compared to $MoSe_2$-CCP (η_{50} ~353 mV and Tafel' slope ~36 mV dec^{-1}), as discussed in **Figure 4.2** of chapter 4. The good HER and OER activities of in-situ binder free electrodes make them suitable bifunctional catalysts for overall water splitting. This study delves into examining the electrochemical response and faradaic efficiency of binder free in-situ grown $MoSe_2$ electrode ($MoSe_2$-CCP and $MoSe_2$-Ni foam) based alkaline electrolyzer. To study the performance of designed electrolyzers, we have conducted LSV and chronoamperometry studies.

5.6.1.1 Performance of electrolyzer for overall water splitting

The good HER and OER activity of prepared binder-free electrodes make them suitable bifunctional catalysts for overall water splitting. The Faradic efficiency is a crucial parameter for evaluating the electrocatalytic performance of a catalyst in OER or HER for overall water splitting. We have performed the two-electrode overall water-splitting using an indigenously designed alkaline water electrolyzer with 1M KOH solution. The binder free $MoSe_2$-CCP and $MoSe_2$-Ni foam electrodes (1 cm^{-2} each) are employed as electrodes symmetrically, while PVA-KOH is used as an electrolyzer membrane. The $MoSe_2$-CCP based electrolyzer shows η_{10} ~370 mV, while $MoSe_2$-Ni foam based electrolyzer exhibits η_{10} ~335 mV at room temperature, as shown in **Figure 5.3 (a)**, suggesting better water spilling response of $MoSe_2$-Ni foam based electrolyzer. **Figure 5.3 (b)** shows the chronoamperometry responses of both electrolyzers, suggesting better stability of $MoSe_2$-Ni foam-based electrolyzer. Further, the amount of gases evolved (H_2 and O_2) have been measured experimentally and calculated theoretically **(using equation 5.2, 5.3)**, as shown in **Figure 5.3 (c, d)**. The faradaic efficiencies

of $MoSe_2$-CCP and $MoSe_2$-Ni foam electrodes for H_2 and O_2 evolution in water splitting electrolyzers are shown in **Figure 5.3 (e)** and **Figure 5.3 (f)**, respectively. The $MoSe_2$-Ni foam based electrolyzer shows better faradaic efficiency for H_2 (~96%) and O_2 (~96%) compared to $MoSe_2$-CCP (H_2 ~93% and O_2 ~91%) after 100 minutes of gas collection.

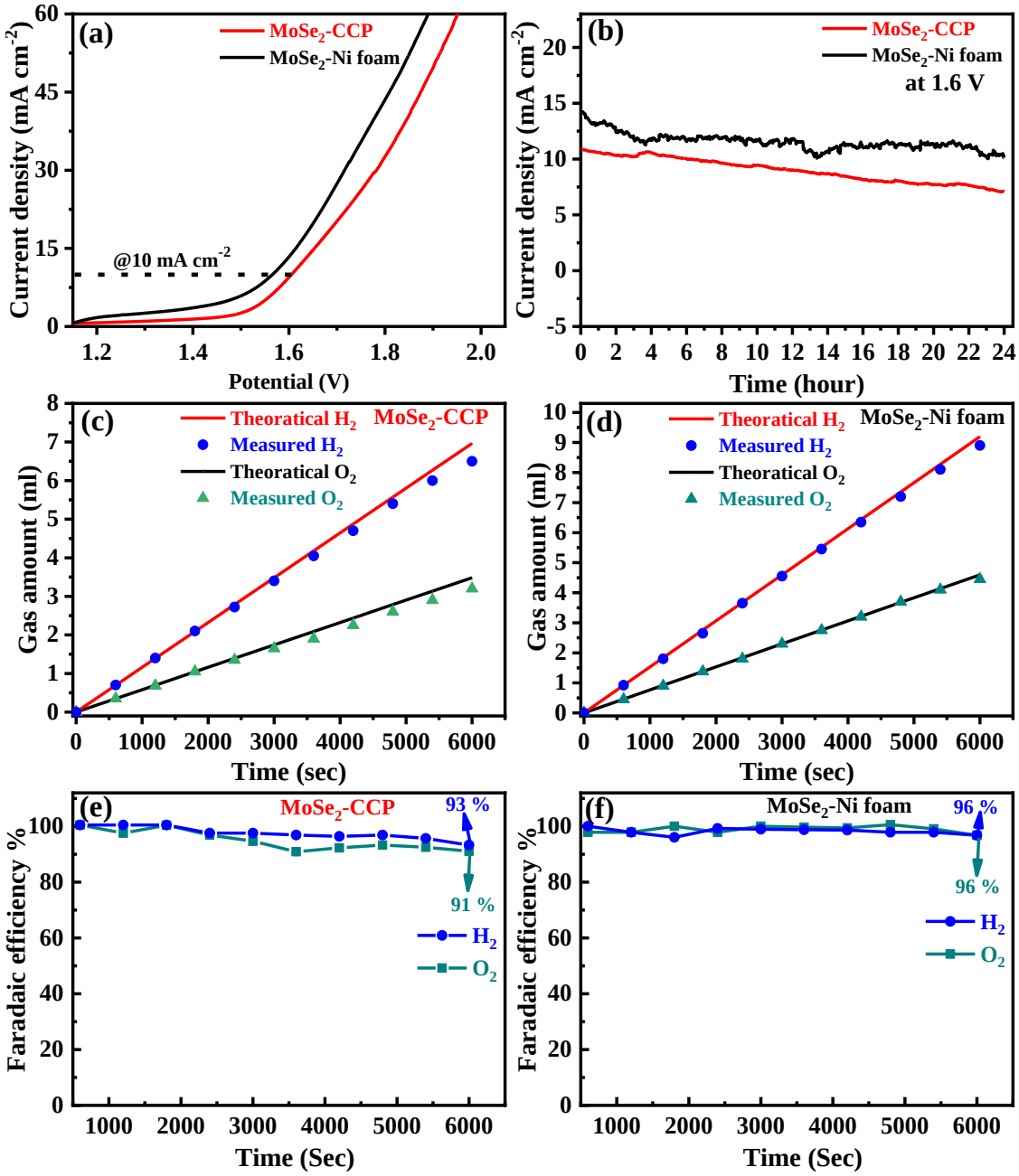

Figure 5.3 *Performance of $MoSe_2$-CCP and $MoSe_2$-Ni foam based electrolyzers, (a) LSV curves at a potential scan rate of 2 mVs^{-1}, (b) chronoamperometric measurement at a constant potential of 1.6 V vs RHE, theoretically calculated and experimentally measured H_2 and O_2 gas vs time for overall water splitting with (c) $MoSe_2$-CCP and (d) $MoSe_2$-Ni foam based electrolyzers; Faradaic efficiency of (e) $MoSe_2$-CCP, (f) $MoSe_2$-Ni foam based electrolyzers for H_2 and O_2.*

5.6.2 Pristine $MoSe_2$ nanosheets as electrode for alkaline water electrolyzer

In this study, we have explored the hydrothermally synthesized pristine $MoSe_2$ nanosheets powder coated on CCP as electrodes for alkaline water electrolyzer. SEM and TEM images of pristine powder suggest the formation of interconnected wrinkled few layer nanosheets morphology and each nanosheets stack contain 6-7 layers, as shown in **Figure 3.9** of chapter 3. The XRD pattern, Raman and FTIR spectra have been discussed in **Figure 3.10** of chapter 3, confirming the 2H phase formation of $MoSe_2$**.** The XPS analysis confirms the existence of characteristic peaks of Mo 3d, Se 3d, as shown in **Figure 3.11** of chapter 3. The OER study of pristine $MoSe_2$ shows overpotential η_{10} of ~391 mV and Tafel's slope of ~78 mV dec^{-1}, (**Figure 4.4 (e)** of chapter 4). Similarly, pristine $MoSe_2$ shows the significant HER (η_{10} ~165 mV and Tafel's slope ~294 mV dec^{-1}) activity. The significant HER and OER activity of pristine $MoSe_2$ nanosheets powder make it suitable bifunctional catalyst for overall water splitting. This study delves into examining the electrochemical water splitting response of pristine $MoSe_2$ electrodes based water electrolyzer. To study the performance of electrolyzer, we conducted LSV and chronoamperometry studies.

5.6.2.1 Performance of electrolyzer for overall water splitting

In this study, we have performed the two-electrode overall water-splitting using our designed alkaline electrolyzer with 1M KOH solution. The pristine $MoSe_2$ nanosheets electrodes (1 cm^{-2} each) are employed as electrodes symmetrically, while PVA-KOH is used as an electrolyzer membrane. The pristine $MoSe_2$ based electrolyzer shows η_{10} ~560 mV, as shown in **Figure 5.4 (a)**, suggesting significant electrocatalytic performance of electrolyzer. **Figure 5.4 (b)** shows the chronoamperometry responses of electrolyzer, suggesting high stability of pristine $MoSe_2$ nanosheets based electrolyzer. Further, the amount of gases (H_2 and O_2) evolved, have been measured experimentally and calculated theoretically **(using equation 5.2, 5.3)**, as shown in **Figure 5.4 (c, d)**. The faradaic efficiencies of pristine $MoSe_2$ nanosheets

based electrolyzer for H_2 and O_2 evolution are shown in **Figure 5.4 (e)** and **Figure 5.4 (f)**, respectively. The pristine $MoSe_2$ based electrolyzer shows good faradaic efficiency for H_2 (~83%) and O_2 (~82%) after 100 minutes of gas collection.

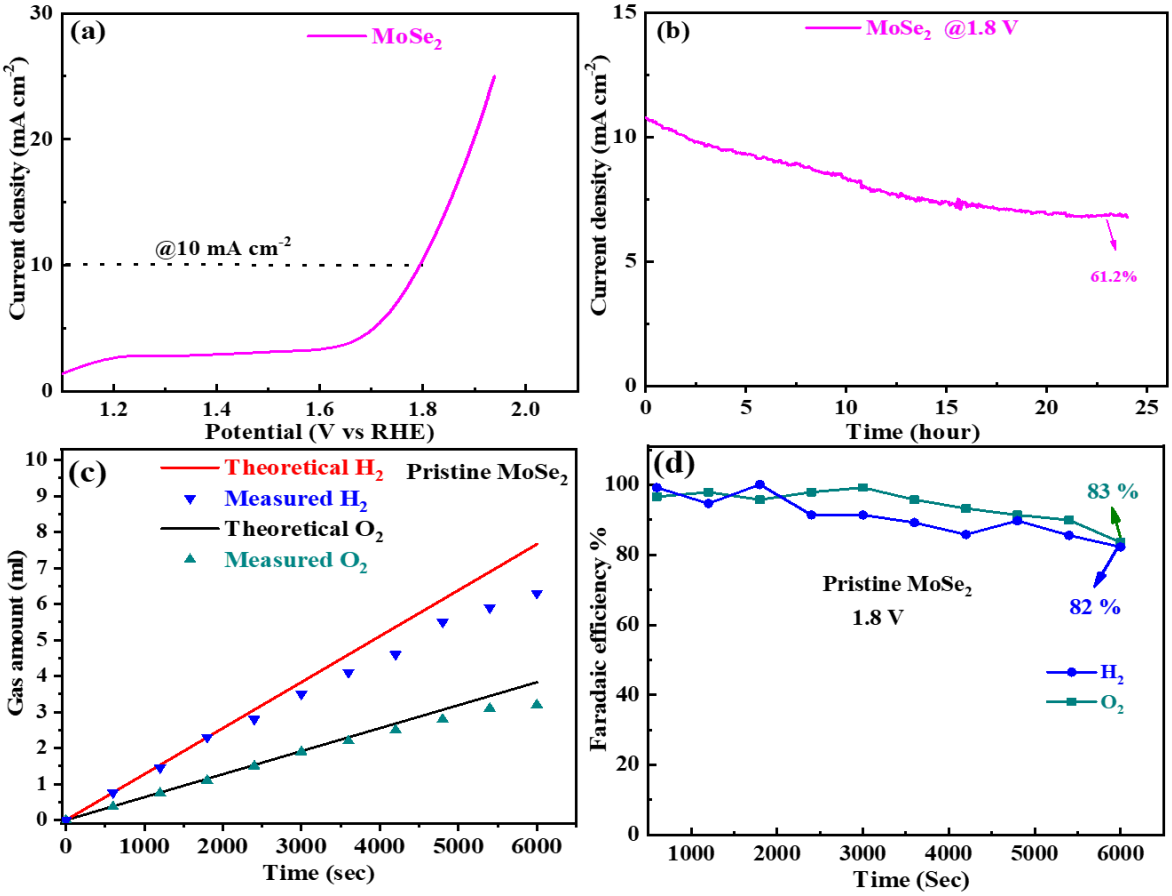

Figure 5.4 *Performance of pristine $MoSe_2$ based electrolyzer, (a) LSV curves at a potential scan rate of 2 mVs^{-1}, (b) chronoamperometric measurement at a constant potential of 1.6 V vs RHE, (c) theoretically calculated and experimentally measured H_2 and O_2 gas vs time for overall water splitting and (d) Faradaic efficiency of electrolyzers for H_2 and O_2.*

5.6.3 Ni decorated $MoSe_2$ nanosheets as electrode for alkaline water electrolyzer

In this study, we have explored the hydrothermally synthesized Ni decorated over $MoSe_2$ (Ni-$MoSe_2$ (5%), Ni-$MoSe_2$ (10%) and Ni-$MoSe_2$ (20%) nanocomposites) as bifunctional electrocatalysts for electrochemical electrolyzer. SEM study of Ni-$MoSe_2$ nanocomposites shows the existence of uniformly distributed Ni nanoparticles on $MoSe_2$ nanosheets for all prepared materials and indicate the existence of uniformly distributed Ni nanoparticles on $MoSe_2$

nanosheets for all prepared nanocomposites (**Figure 3.14** of chapter 3). TEM study (**Figure 3.15** of chapter 3) illustrates the formation of Ni nanoparticles on the $MoSe_2$ nanosheets in Ni-$MoSe_2$ (10%) nanocomposite. The XRD, Raman, and FTIR studies of confirm the various phase of Ni-$MoSe_2$ nanocomposites (Figure 3.16 of chapter 3). The XPS analysis of Ni-$MoSe_2$ (10%) has confirmed the presence of Mo3d, Se3d and Ni 2p (**Figure 3.17** of chapter 3**)**. The ECSA study has shown that Ni-$MoSe_2$ (10%) has higher C_{dl} value of 32.2 mF cm^{-2} compared to Ni-$MoSe_2$ (5%) (23 mF cm^{-2}) and Ni-$MoSe_2$ (20%) (29 mF cm^{-2}). The Ni-$MoSe_2$ nanocomposites have also been investigated for HER in 1M KOH (**Figure 3.19** of chapter 3). The performance of HER reveals that the Ni-$MoSe_2$ (10%) nanocomposite exhibits lower η_{10} ~141 mV and Tafel slope ~60 mV dec^{-1} compared to Ni-$MoSe_2$ (20%) (η_{10} ~ 163 mV, Tafel slope ~76 mV dec^{-1}) and Ni-$MoSe_2$ (5%) (η_{10} ~ 170 mV, Tafel slope ~84 mV dec^{-1}). Similarly, for OER study, Ni-$MoSe_2$ (10%) nanocomposites shows better OER performance with η_{10} ~277 mV and Tafel slope ~53 mV dec^{-1} as compared to Ni-$MoSe_2$ (20%) (η_{10} ~ 293 mV, Tafel slope ~57 mV dec^{-1}), Ni-$MoSe_2$ (5%) (η_{10} ~ 306 mV, Tafel slope ~ 66 mV dec^{-1}). The good HER and OER activity of Ni-$MoSe_2$ nanocomposites make it suitable bifunctional electrocatalyst for overall water splitting. This alkaline water electrolyzer study delves into examining the electrochemical water splitting response of Ni-$MoSe_2$ nanocomposites based electrodes. To study the performance of the electrolyzer, we conducted studies using LSV and chronoamperometry studies.

5.6.3.1 Performance of electrolyzer for overall water splitting

The good HER and OER activity of prepared Ni-$MoSe_2$ nanocomposites based electrodes make them suitable bifunctional catalyst for overall water splitting. Further, we have performed the two-electrode overall water-splitting by using our designed alkaline electrolyzer with 1M KOH solution. The Ni-$MoSe_2$ nanocomposites (1 cm^{-2} each) are employed as electrodes symmetrically, while PVA-KOH is used as an electrolyzer membrane. The Ni-$MoSe_2$ (10%) based electrolyzer shows lower overpotential of η_{10} ~284 mV compared to Ni-

$MoSe_2$ (5%) exhibiting η_{10} ~449 mV and Ni-$MoSe_2$ (20%) showing η_{10} ~364 mV at room temperature, as shown in **Figure 5.5 (a)**. It suggests better electrocatalytic performance of Ni-$MoSe_2$ (10%) based electrolyzer. **Figure 5.5 (b)** shows the chronoamperometry responses of Ni-$MoSe_2$ based electrolyzers, suggesting Ni-$MoSe_2$ (10%) nanocomposites based electrolyzer has better stability (~86.2% of current retention) at constant potential 1.6 V vs RHE compared Ni-$MoSe_2$ (5%) (~62.8% of current retention), and Ni-$MoSe_2$ (20%) (~75.5% of current retention). Further, the amounts of gases (H_2 and O_2) evolved, have been measured experimentally and calculated theoretically **(using equation 5.2, 5.3)**, as shown in **Figure 5.5 (c)** for Ni-$MoSe_2$ (5%), **Figure 5.5 (d)** for Ni-$MoSe_2$ (10%) and **Figure 5.5 (e)** for Ni-$MoSe_2$ (5%) nanocomposites. The faradaic efficiencies of Ni-$MoSe_2$ (5%), Ni-$MoSe_2$ (10%), and Ni-$MoSe_2$ (20%) electrodes for H_2 and O_2 evolution in water splitting electrolyzers are shown in **Figure 5.5 (f)**, **Figure 5.5 (g) and Figure 5.5 (h)**, respectively. The Ni-$MoSe_2$ (10%) based electrolyzer shows better faradaic efficiency for H_2 (~93%) and O_2 (~93%) compared to Ni-$MoSe_2$ (5%) (H_2 ~81% and O_2 ~75%) and Ni-$MoSe_2$ (20%) (H_2 ~84% and O_2 ~83%) after 100 minutes of gas collection. Performance of all studied electrolyzer with different electrodes like binder-free electrodes ($MoSe_2$-CCP and $MoSe_2$-Ni foam), pristine $MoSe_2$, and Ni decorated over $MoSe_2$ (Ni-$MoSe_2$ (5%), Ni-$MoSe_2$ (10%) and Ni-$MoSe_2$ (20%)) nanocomposites with 1M KOH have been summarized in **Table 5.1**.

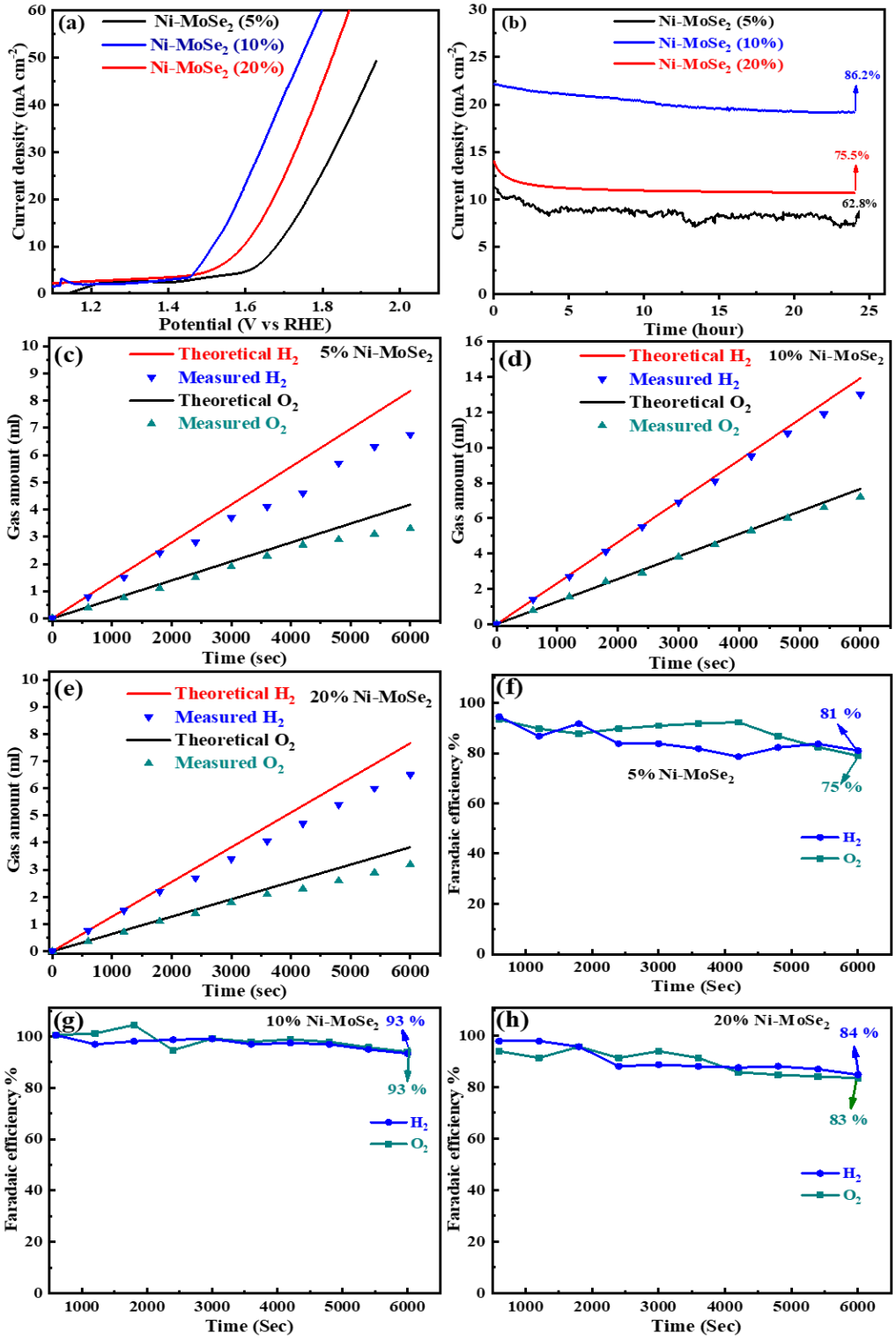

Figure 5.5 *Performance of Ni-MoSe₂ (5%), Ni-MoSe₂ (10%) and Ni-MoSe₂ (20%) based electrolyzers, (a) LSV curves at a potential scan rate of 2 mVs^{-1}, (b) chronoamperometric measurement at a constant potential of 1.6 V vs. RHE; theoretically calculated and experimentally measured H_2 and O_2 gas vs time for overall water splitting with (c) Ni-MoSe₂ (5%), (d) Ni-MoSe₂ (10%) and (e) Ni-MoSe₂ (20%) based symmetric electrolyzers; Faradaic efficiency of (f) Ni-MoSe₂ (5%), (g) Ni-MoSe₂ (10%) and (h) Ni-MoSe₂ (20%) nanocomposites based electrolyzers for H_2 and O_2.*

Table 5.1 The comparative electrolyzer performance using our studied materials.

Electrocatalysts	Overpotential η_{10} (mV)	Electrolyte	Faradaic efficiency	
			H_2	O_2
$MoSe_2$-CCP	**370**	1M KOH	***93***	91
$MoSe_2$-Ni foam	**335**	**1M KOH**	***96***	**96**
$MoSe_2$	560	1M KOH	***83***	**82**
Ni-$MoSe_2$ (5%)	449	1M KOH	**81**	75
Ni-$MoSe_2$ (10%)	**284**	**1M KOH**	**93**	**93**
Ni-$MoSe_2$ (20%)	364	1M KOH	**84**	83

5.7 Conclusion

This chapter discusses about the performance of alkaline water electrolyzer with binder-free electrodes ($MoSe_2$-CCP and $MoSe_2$-Ni foam), pristine $MoSe_2$, and Ni decorated over $MoSe_2$ (Ni-$MoSe_2$ (5%), Ni-$MoSe_2$ (10%) and Ni-$MoSe_2$ (20%)) nanocomposites based electrolyzer with 1M KOH. Binder-free $MoSe_2$-Ni foam shows a low overpotential of 335 mV at a current density of 10 mA cm^{-2} with faradaic efficiency for H_2 (~96%) and O_2 (~96%) compared to $MoSe_2$-CCP (η_{10} ~370 mV, Faradaic efficiency for H_2 ~93% and O_2 ~91%). High electrolyzer performance for $MoSe_2$-Ni foam electrode is due to its individual high HER (discussed in chapter 3) and OER (discussed in chapter 4) activities, attributed to high catalytic kinetics, high catalytic sites due to vertical orientation of $MoSe_2$, high electrocatalytic durability and low charge transfer resistance. Among Ni-$MoSe_2$ nanocomposites and pristine $MoSe_2$, Ni-$MoSe_2$ (10%) shows a lowest overpotential of 284 mV at a current density of 10 mA cm^{-2} with faradaic efficiency for H_2 (~93%) and O_2 (~93%) compared to Ni-$MoSe_2$ (5%) (η_{10} ~449 mV, Faradaic efficiency for H_2 ~81% and O_2 ~75%), Ni-$MoSe_2$ (20%) (η_{10} ~364 mV, Faradaic efficiency for H_2 ~84% and O_2 ~83%) and pristine $MoSe_2$ (η_{10} ~560 mV, Faradaic efficiency for H_2 ~83% and O_2 ~82%). High electrolyzer performance for Ni-$MoSe_2$ (10%)

based electrode is due to its individual high HER (discussed in chapter 3) and OER (discussed in chapter 4) activities, attributed to high catalytic kinetics, high electrical conductivity, high catalytic active sites due to Ni decoration over $MoSe_2$, and high synergistic effect between $MoSe_2$ and Ni nanoparticle in Ni-$MoSe_2$ nanocomposites.